

MAGNETOTRANSPORT IN QUASILATTICES

UWE GRIMM, FLORIAN GAGEL, MICHAEL SCHREIBER
Institut für Physik, Technische Universität, D-09107 Chemnitz, Germany

The dc conductance and the Hall voltage of planar arrays of interconnected quantum wires are calculated numerically. Our systems are derived from finite patches of aperiodic graphs, with completely symmetric scatterers placed on their vertices which are interconnected by ideal quantum wires. Already in a periodic square lattice arrangement, quantum interference effects lead to complicated magnetotransport properties related to the Hofstadter butterfly. For rectangular Fibonacci grids and other quasiperiodic lattices, we obtain still more complex fractal patterns. In particular, irrational ratios of edge lengths and of tile areas in our samples destroy the periodicities with respect to the Fermi wave vector and the magnetic flux, respectively.

1 Introduction

Phase-coherent quantum transport manifests itself through many exciting phenomena. The observation of conductance quantization, the Aharonov-Bohm effect, universal conductance fluctuations, and other interference effects in mesoscopic systems (see, e.g., Ref. 1 for an overview) has been made possible by the technological advance in device fabrication. In this domain, macroscopic properties like conductance and Hall voltage critically depend on the interference of multiply scattered waves. Principally, this opens up the possibility to extract information about a system through *conductance spectroscopy*, i.e., by observing its transport properties upon variation of the microscopic interference pattern, for instance via an external magnetic field.

Even in a simple periodic structure, the presence of a magnetic field leads to complicated fractal spectra. A well-known example is the famous Hofstadter butterfly² which describes the eigenvalue spectrum of electrons in a periodic lattice subject to a perpendicular magnetic field. Here, we investigate phase-coherent magnetotransport in quasiperiodic structures. As model systems, we choose Fibonacci grids and finite quadratic patches of the ideal octagonal Ammann-Beenker tiling (compare Fig. 1). While related work is mostly based on a tight-binding approach,^{3–5} we follow Ref. 6 and consider an ensemble of interconnected scatterers that are linked by ideal waveguides. The advantage is that we do not depend on the details of the leads that have to be specified for any open tight-binding system. Our approach can be seen as a “strong confinement” limit, where one-dimensional electron motion is possible only on straight, ideal connection lines between the crossings.

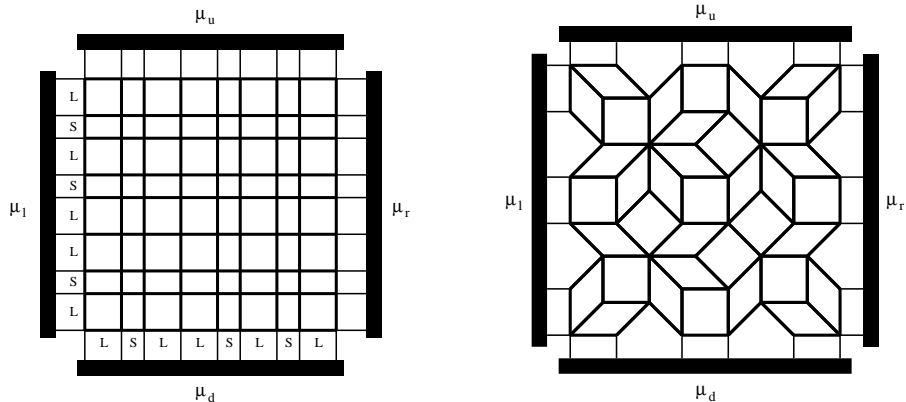


Figure 1: Geometry of our systems: Fibonacci grid (left) and octagonal approximant (right).

2 Numerical approach

We consider quadratic systems connected to four electron reservoirs (terminals), see Fig. 1. Assuming small driving voltages (applied between the left and right terminals, the “up” and “down” contacts serving as voltage probes), we have a linear relation between currents and chemical potentials of the contacts,

$$I_\alpha = \frac{2e}{h} \sum_\beta T_{\alpha\beta} \mu_\beta \quad (\alpha, \beta \in \{l, r, u, d\}) \quad (1)$$

where I_α is the outgoing current at terminal α and μ_β denotes the chemical potential of terminal β . This system of equations has to be solved while ensuring current conservation in the voltage probes. The voltage between two contacts is related to the difference in their chemical potentials by $eU_{\alpha\beta} = \mu_\beta - \mu_\alpha$.

In the Landauer-Büttiker description,⁷ the transmission matrix T is obtained from the *scattering matrix* S . First, we consider a node connecting N waveguides. In order to describe the scattering process at such a crossing, we use a symmetric $N \times N$ scattering matrix S_N with diagonal elements (backscattering amplitudes) r and off-diagonal elements (transmission amplitudes) t . Neglecting spatial extension, assuming time-reversal symmetry and demanding unitarity implies $t = 2/N$ and $r = t - 1$. In the limit of a continuum of scattering channels, S_N corresponds to isotropic S -wave scattering.

Now, we consider a pair of adjacent linked nodes j and k . A wave outgoing from node k acquires a phase factor $P_{jk} = \exp[i(qa_{jk} + \varphi_{jk})]$ along the waveguide between the two nodes. Here, q denotes the modulus of the wave vector,

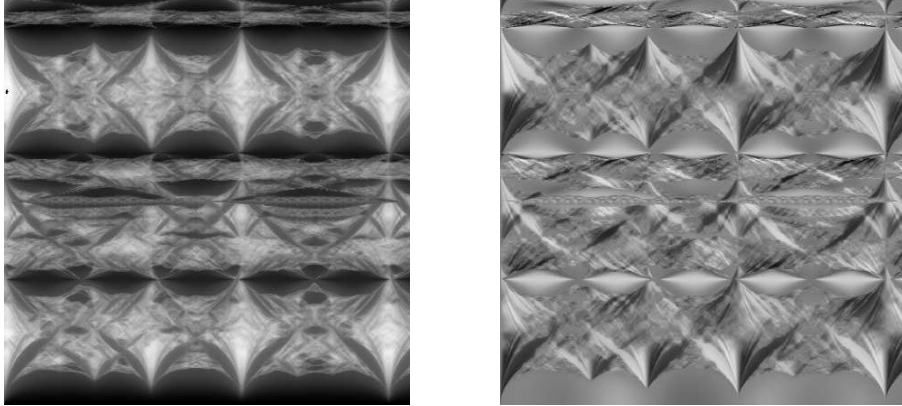


Figure 2: Conductance (left) and Hall voltage (right) for a Fibonacci grid as a function of the wave vector q (vertically from 0 to 2π) and the magnetic flux Φ in units of the flux quantum h/e (horizontally from 0 to 2). On the left side, the conductance vanishes in the dark regions and increases with the brightness. In the right plot, the Hall voltage is negative in the dark parts and positive in the bright regions.

and $a_{jk} = a_{kj}$ measures the distance between the two nodes. The contribution $\varphi_{jk} = \frac{e}{\hbar} \int_k^j \vec{A} \cdot d\vec{s}$ accounts for the additional phase shift due to the magnetic field, and the Landau gauge can be used for the vector potential: $\vec{A} = By\vec{e}_x$.

In order to obtain the *overall* scattering matrix S from the S_N and P_{jk} , we use the approach presented in Ref. 6 to sum up all the multiple interferences in the system. Then we solve Eq. (1) under the condition of current conservation in the two voltage contacts ($I_u = I_d = 0$). This yields the magnetoconductance $G = I/U$, $I = I_l = -I_r$ being the total current and $U = U_{rl}$ the voltage measured between source and drain contact, as well as the Hall conductance $G_H = I/U_H$, where $U_H = U_{ud}$ is measured between the two voltage probes.

3 Results

In Fig. 2, the conductance and the Hall voltage for a Fibonacci grid with $14^2 = 196$ scatterers is shown as a function of the wave vector and the magnetic flux. The Fibonacci grid contains edges of two different lengths [1 and the golden mean $\tau = (1 + \sqrt{5})/2$] and tiles of three different areas (1, τ and $\tau^2 = \tau + 1$). Fig. 3 shows the Hall voltage for an octagonal patch with 264 scatterers. Here, all edges have the same length (which we choose to be 1), wherefore the conductance and the Hall voltage are periodic in the wave vector q with period π . However, the tile areas are incommensurate (the squares

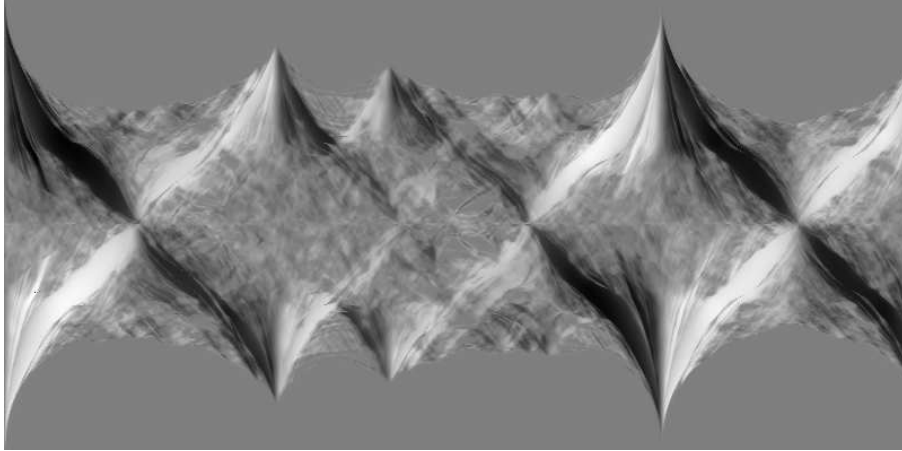


Figure 3: Hall voltage for an octagonal patch as a function of the wave vector q (vertically from 0 to π) and the magnetic flux (horizontally from 0 to 4). The shading is as indicated in Fig. 2. Note the almost perfect antisymmetry with respect to $q = \pi/2$.

have an area of 1, the rhombs an area of $1/\sqrt{2}$, i.e., one has no periodicity in the magnetic flux. Note that the result for the Fibonacci grid is not periodic in either variable. Nevertheless, the figures are reminiscent of the square lattice case.⁶ In particular, one clearly recognizes distinctive structures in the transport properties of both systems, consisting of patterns that are repeated quasiperiodically. A more detailed analysis of these features will be presented elsewhere.

An experimental verification of our results could be based on a system of interconnected small quantum wires in an appropriate setup at sufficiently low temperatures to maintain phase coherence all over the structure.

References

1. B. Kramer (ed.), *Quantum Coherence in Mesoscopic Systems* (Plenum, New York 1991).
2. D.R. Hofstadter, *Phys. Rev. B* **14**, 2239 (1976).
3. K. Ueda and H. Tsunetsugu, *Phys. Rev. Lett.* **58**, 1272 (1987).
4. T. Hatakeyama and H. Kamimura, *Solid State Communications* **62**, 79 (1987); *J. Phys. Soc. Japan* **58**, 260 (1989).
5. G. Kasner, H. Schwabe, and H. Böttger, *Phys. Rev. B* **51**, 10454 (1995).
6. F. Gagel and K. Maschke, *Phys. Rev. B* **49**, 17170 (1994).
7. M. Büttiker, *Phys. Rev. Lett.* **57**, 1761 (1986).